MICROSTRUCTURE AND PROPERTIES OF EXTRUDED SHS MATERIALS

T. N. Shishkina, V. V. Podlesov, and A. M. Stolin

UDC 621.762:621.7.011

Experimental results are presented on the microstructure and some properties of composite refractory materials fabricated by the SHS method under subsequent shear deformation (extrusion).

A fundamental specific feature of a new technology for producing articles from refractory materials, called SHS extrusion [1], consists in using the favorable strain distribution and shear plastic deformation of the material.

It is known that the high-pressure effect on the structure and mechanical properties of solids under deformation is strong and, in the majority of cases, favorable: the titanium structure changes under compression (a system of dark bands is formed in the directions of maximum shears) [2], the strength and plasticity of brittle materials increase under rolling and other types of pressing [3], cracks and voids in the material under deformation are "healed" [4], grain refinement takes place, and a highly uniform structure under hydroextrusion of metals [5] is attained.

As is known, plastic deformation often results in the formation of textured anisotropic materials, which is the cause of their improved mechanical characteristics and sometimes the appearance of unique properties [5].

So, for example, results on improving the strength density and hardness of metals exposed to cold hydroextrusion are available. It is interesting that at the same time the plasticity (~10 times) of such brittle, not easily deformed materials as molybdenum and tungsten has increased. In addition, the molybdenum microstructure (marked grain elongation) has substantially changed; after hydroextrusion a molybdenum rod is capable of being coiled while the basic (hot-pressed) material fails by bending through an angle of 3-8°.

Also, a method of achieving the assigned anisotropy of properties that provides high endurance of bearing rings is known [6]. Such anisotropy of the properties can be determined by special rolling, as a result of which a metal fiber layer is formed around the workpiece perimeter.

The SHS method ensures both quite new possibilities of fabricating articles from inorganic compounds and a number of interesting specific features of structure formation. The conditions responsible for structural macrokinetics in a self-propagating high-temperature synthesis (SHS) wave and in more low-temperature traditional technologies, particularly in powder metallurgy, are basically different [7]. The short time (of the order of ten seconds) of the process is the reason why this process is nonequilibrium, and stipulates some specific features of structure formation that affect the properties of materials to be produced. For example, in making ferrites and bismuth-containing complex oxides [8], the effect of the anisotropy of the properties due to the combustion wave direction is observed in polycrystal samples.

At present the SHS extrusion method is used to fabricate long articles from refractory materials, including powder composition that are hard to sinter and badly pressed. In this method, the processes of combustion and synthesis coincide with those of shear deformation, thereby giving quite new specific features to the structure formation of materials. Because of this, the problem arises of how to analyze the features that cause considerable shear deformations in the microstructure of articles.

The present work deals with the following characteristics of the microstructure of the extruded articles: shape and size of a hard base; microporosity; distribution of these characteristics along the length and over the cross section of articles; component distribution; flow patterns of the test material based on studying the distribution of these components.

Institute of Structural Macrokinetics, Russian Academy of Sciences, Chernogolovka. Translated from Inzhenerno-Fizicheskii Zhurnal, Vol. 63, No. 5, pp. 547-556, November, 1992. Original article submitted January 9, 1992.

1062-0125/92/6305-1082$12.50

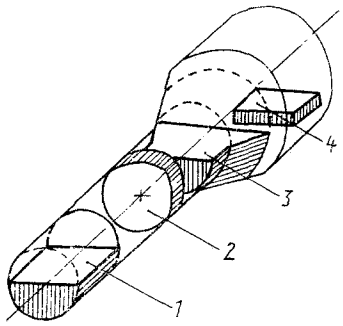

Fig. 1. Cutting the extruded samples into microsections for microstructure study: 1) length microsection of the extruded part; 2) cross microsection of the extruded part; 3) length microsection of the material near the die assembly; 4) length microsection of the material in the container.

I. Features of Structure Formation of Materials under SHS Extrusion and Some Properties of Titanium Carbide Hard Alloy (SHTM) Articles (SHTM-2 Used as an Example). To study the features of structure formation of materials under SHS extrusion a hard alloy of the SHTM-2 group comprising 70 mass % of titanium carbide (TiC) and 30 mass % of nickel binder after synthesis was chosen as a model system. Its microstructure and phase composition were studied earlier as applied to SHTM technology [9].

The extruded samples were cut along and across their axes as shown in Fig. 1. After this, the microsections were manufactured by the standard method. The quantitative phase composition and porosity of samples were examined by the point method [10] from the microstructure photos taken in backward scattered electrons on the JCXA-733 X-ray microanalyzer. A net with sites varying from 850 to 1000 was used at each measurement. In addition, the porosity was determined by the standard scale.

The mean size of the titanium carbide grains was determined by the linear method from the microstructure photos (direct measurements of diameters and largest–smallest images of particles followed by their averaging). Here, the accuracy in determining the particle sizes was 1.5-2%, allowing for the representative sampling. The stereological determination of the actual particle size distribution was made by A. G. Spektor's method [10] from several dozens of measurements.

The structure [9] is characteristic of the test hard alloy: brittle TiC particles (on the photos, the dark grains close, in shape, to spherical ones) located in the viscous metal container, in this case, in the nickel one (on the photos, the light regions surrounding the TiC grains). Such a structure is typical of hard alloy composite materials. These photos illustrate that after synthesis the titanium carbide grains gain the spherical shape to be kept during extrusion. Subsequent calculations have shown that the characteristic grain sizes in an arbitrary direction are approximately the same. Additionally, this points to the spherical similarity of the titanium carbide grains.

To directly observe the shape and size of the TiC grains the extruded samples have been subjected to deep selective nickel etching. Figure 2 clearly illustrates the shape of the grains in the fracture (secondary electron image). The carbide grains are closely pressed against each other, and the characteristic contact areas are formed at the places of their contact.

Measurement of the mean grain size along the sample symmetry axis has shown that in the initial sample part, which appears earlier beyond the deformed zone of the material, the size of the TiC particles is 4.0-4.3 μm, while in the final sample part, which is mostly under strain, it is equal to 3.5-3.7 μm, i.e., the difference is not very great.

More substantial grinding of the titanium carbide grains is observed in the cross direction from the center (3.5-4 μm) to the periphery – 2.6 μm and, in some cases, up to 1.6 μm (Fig. 3). This can be attributed both to rapid cooling of the surface layers because of which the grain growth is hindered, and to the features of the strain distribution under shear deforming. It may also be noted that the mean size of the titanium carbide grains decreases with increasing strain value ψ, which represents the ratio

$$\psi = \frac{d_0^2 - d_1^2}{d_0^2} .$$

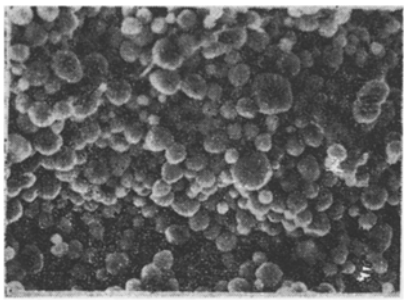

Fig. 2

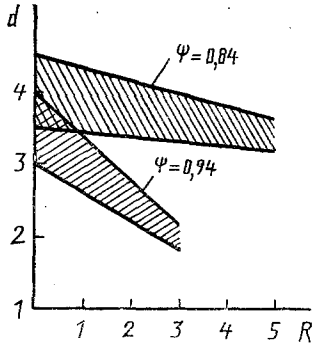

Fig. 3

Fig. 2. Carbide skeleton after selective nickel etching.

Fig. 3. Distribution of the mean titanium carbide grain size d, μm, over the sample radius R, mm, at different strain values ψ.

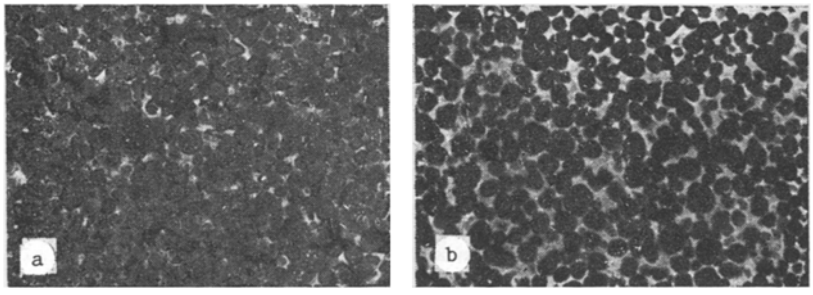

Fig. 4. Microporosity of the extruded samples in cross (a) and length (b) cuts. ×1000.

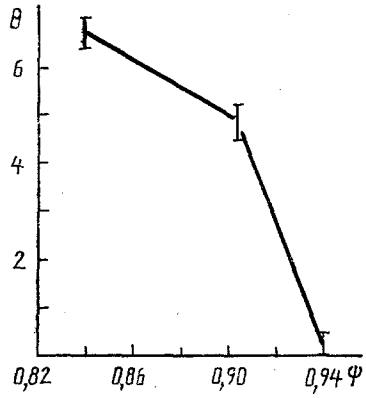

Fig. 5. Microporosity Θ, %, of the samples as a function of strain value.

The microporosity of the articles and the quantitative phase composition were studied by the point method on a net with about 1000 sites. A study of the length and cross cuts of the samples has revealed different values of the microporosity for all test samples. This allows a conclusion to be made about the anisotropy of the porosity under SHS extrusion (Fig. 4). Obviously, it is bound up with the features of deforming a porous extruded workpiece. The remaining pores are located not at random but in the material flow direction. Probably, a greater value of the porosity in the cross direction is attributed to the fact that for such a cut all the pores prove to be in the visual field and for a length cut, only some of them.

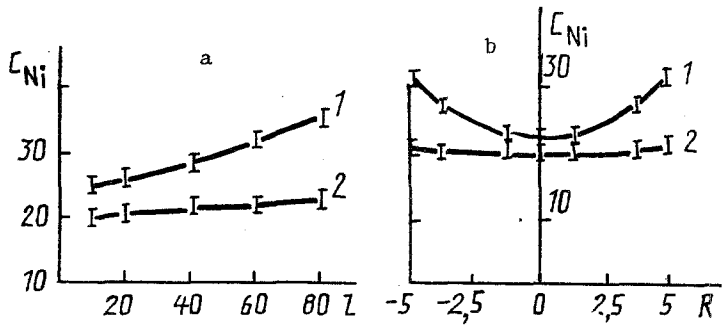

Fig. 6. Distribution of nickel concentration C, vol.%: a) along the sample l, mm [1) ψ = 0.84; 2) 0.94]; b) over the sample radius R, mm [1) at an extrusion temperature of 1900 K; 2) 1700 K].

The photos of the inlet part of the sample taken with small magnification clearly show the pore location (dark points along certain lines coinciding with the material flow direction).* This specific feature of the pore system location under SHS extrusion is a prerequisite to texture formation of materials; in addition, other things being equal, it can have a favorable effect on the strength characteristics of articles. The porosity magnitude is strongly affected by the strain value (Fig. 5). As the strain value increases from 0.84 to 0.94, the value of the porosity θ decreases to fractions of a percent.

Consideration of the volume content of the phases points both to some nonuniformity of the structure due to the redistribution of the nickel binder from the center to the periphery in the cross direction and to somewhat increased volume content at the entrance section (in studies of the length cut). The maximum deviation of the nickel content from the theoretical value is 10-12% in the cross direction and up to 15% in the longitudinal one.

Evidently, the specific features of deformation of a workpiece burnt in the container are the reason for such a redistribution. As the calculations show [11], near the outlet of the container there always exists a temperature gradient due to strong heat removal to the container. The material layers cooled to different temperatures are packed not uniformly. The material near the container walls has the highest porosity.

If, when deforming the workpiece, the nickel binder is in a liquid state, then under external pressure it is extruded into the elevated porosity regions. Thus, the nonuniform distribution of the binder in diameter appears, as well as nickel binder enrichment of the entrance sections of the articles which also have the elevated porosity.

Control of these phenomena may follow two directions. The first means an increase of the strain value, thus reducing the porosity of the article. So, by increasing ψ from 0.84 to 0.94 a marked decrease of the nonuniform distribution of the phase composition along the article (Fig. 6a) has been gained. The second relates to the choice of an optimal extrusion temperature range [12]. For example, if we have begun extrusion at a temperature below the melting point of the metal-binder (in this case, nickel with T_{melt} = 1720 K), we can obtain a metal-binder distribution along the sample (Fig. 6b) practically uniform and close to the theoretical one.

To study the flow pattern of the material in the container we have adopted the sandwich sample method based on using zirconium dioxide (ZrO_2) powder. ZrO_2 has been chosen for the following reasons: Its melting point (3000 K) is higher than the combustion one (2300 K) of the composition under consideration, and it is a good substance in studies of a microsection under cathode luminescence. The results on the extruded sandwich samples are shown in Fig. 7.

The system of microcracks is clearly seen both on the remaining part of the material in the container and on the extruded part of the samples. The microcracks are located in the form of parabolas enclosed into one another. Study of the microsections under "compo" and cathode luminescence has shown that these microcracks contain zirconium dioxide, which in the initial workpiece is located in the form of flat layers (Fig. 7a). Thereby, the distribution obtained reflects the final position of the primarily flat ZrO_2 layers after deformation.

*Such a pattern was observed in studies of titanium under deformation [2]: There were strongly deformed zones with clearly pronounced shear bands in materials.

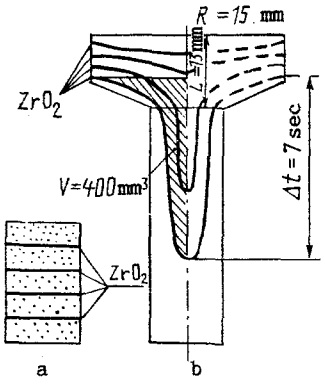

Fig. 7

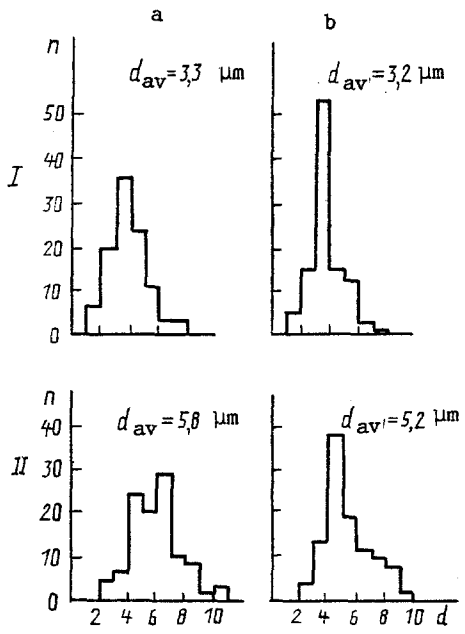

Fig. 8

Fig. 7. Study of the material flow pattern by sandwich sample method: a) initial workpiece; b) zirconium dioxide distribution in the extruded sample.

Fig. 8. Size distribution of the TiC particles for the materials SHTM-2/30N (I) and SHTM-2/20N (II): a) at the sample center; on the b) sample surface. d, μm.

It may be noted that extrusion of the workpiece is substantially irregular in nature. The central material layers are extruded far ahead of the external ones, which are decelerated by the container walls due to friction. Near the surface of the outlet eye the stagnation zones are formed, the material of which does not participate in the motion, evidently because of the ability to deform.

After the extruded molybdenum sample has been examined, the effective viscosity of the test composite material has been approximately estimated at the extrusion moment, amounting to $\eta_{eff} \sim 10^{10}$ Pa·sec = 10^{11} P. Thus, the test material may be considered as a high viscous system filled with hard titanium carbide particles.

In addition to the model composition of SHTM-2 containing 30% of nickel, the microstructure of which has been detailed above, a study has also been made of SHTM-2 comprising 20% of nickel binder. In this situation, the articles have been fabricated, with their diameters ranging from 5 to 10 mm and 2 to 5 mm.

The microstructure of the composition of SHTM-2/20N is identical to that of SHTM-2/30N: rounded titanium carbide grains surrounded by the nickel binder. The differences indicate that for SHTM-2/30N the mean size of grains constitutes 3-3.5 μm, while for SHTM-2/20N, it is 5-6 μm. The side distribution of the TiC particles is shown in Fig. 8. The mean size of the grain from the center to the surface of the sample decreases insignificantly. In addition, the difference in the grains somewhat diminishes. Most likely these phenomena are determined by more rapid cooling of the surface layers of the extruded articles. Thus, to make a fine-grained structure with a maximum size distribution of grains over a narrow range it may be recommended that the material be quenched immediately after its extrusion. Moreover, not only the structure of the fabricated articles but also some of their properties have been examined (Table 1). Such an integral characteristic as specific electrical resistance has been chosen to make nondestructive control of the nonuniformity of the articles produced. The measurement results on this characteristic at room temperature are also shown in Table 1.

Among the mechanical properties of the fabricated articles, we have studied the hardness and bending strength, which are traditionally considered to be the basic characteristics of hard alloys.

As is seen from Fig. 9, the hardness vs article radius and length correlates with the nickel distribution in the sample volume. The obtained values of the bending strength (Fig. 10) relate directly to the round samples of equal length but of different diameter. This is attributed to the fact that for standard tests the 5 × 5 × 35 mm samples cannot be fabricated from cylindrical articles less than 8 mm in diameter.

TABLE 1. Some Characteristics of Articles

Material	Density, g/cm^3	Rockwell hardness	Mean grain size, μm	Specific electrical resistance μΩ·cm
SHTM -2/30H	5,8±9,5%	79±2,3%	3—3,5	57,7±8%
SHTM- 2/20H	5,56±4,3%	80±4%	5—6	73,3±12,6%

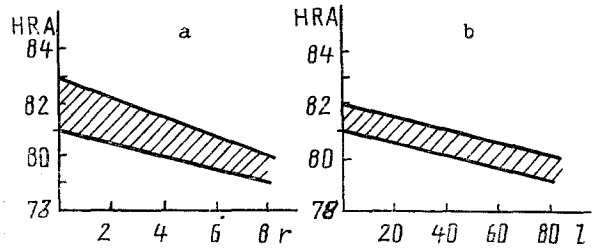

Fig. 9. Hardness vs radius (a) and length (b) of the articles. r, mm.

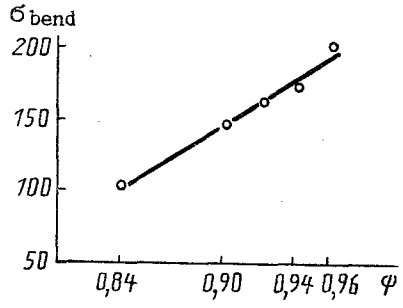

Fig. 10. Bending strength σ, kg/mm^2, as a function of strain value.

By increasing the strain value from 84 to 94%, the bending strength grows from 110 to 220 kg/mm^2. This can be explained by reducing the porosity of the article, its macrononuniformity, as well as by improving the surface quality.

II. Material Texture Formation under Deformation (Hf—Ti—B—Ni System Used as an Example). We have studied the possibilities of the material to form texture under deformation by SHS extrusion of hafnium diboride- and titanium-base materials having nickel binder (Table 2) [13]. The choice of this composite material is determined first of all by the presence of grains having a size that allows its microstructure to be revealed.

Depending on the content of nickel binder in the material (20-40%), the test compositions are denoted by 1, 2, 3, respectively, in Tables 2 and 3.

The microstructure and phase composition of the fabricated materials have been analyzed by using the above methods.

The grains of material Nos. 1 and 2, as a rule, are shaped as elongated "small sticks," which is characteristic of many boride systems. The mean grain size in the material No. 2 sample cross section is, for example, length 2.5 μm; thickness 0.6 μm. Apart from the elongated grains, irregular-shaped ones are encountered; however, their percent content is not great.

In examining the longitudinal cross section of samples of all compositions in the photos taken with small magnification, two types of macroregions have been revealed: dark and light. In material No. 1 with a small content of a binder (20%) the light regions are present in the form of random spots. In material Nos. 2 and 3 with a large content of a binder (30 and 40%), the light and dark regions are located in the form of alternating bands elongated in the material flow direction. Thus, we are dealing here with a clearly defined texture anisotropy of the extruded SHS materials. This result has proved to be fundamentally new for SHS extrusion since earlier we have succeeded in revealing only the orientation of the pore system in the extrusion direction.

TABLE 2. Characteristics of the Charge Compositions Used

Material No.	Content of initial powders in charge, %				Design material composition, %			X-ray phase composition of hard base
	Hf	Ti	B	Ni	HfB_2	TiB_2	Ni	
1	62,4	6,9	10,7	20	70	10	20	(Hf, Ti)B_2
2	53,5	6,9	9,6	30	60	10	30	(Hf, Ti)B_2
3	35,7	13,8	10,5	40	40	20	40	HfB_2, TiB_2

TABLE 3. Characteristics of the Grains in the Test Materials

Material No.	Region	Mean grain length, μm	Mean grain thickness, μm	Elongated-to-total number ratio, %	Oriented-to-elongated grain number ratio, %
1	Dark	3,3	0,9	73	60
	Light	2,0	0,65	53	No orientation
2	Dark	3,8	0,9	81	80
	Light	1,9	0,7	63	No orientation
3	Four-phase	0,8	0,5	53	No orientation

It should be noted that similar effects have been observed at hydroextrusion of metal materials [5]. Usually texture anisotropy of the extruded materials has pure mechanical reasons bound up with the specific features of the strain distribution and shear plastic deformation (extrusion). Apparently, the same reasons are also valid in our case and, unlike [9], the thermal factors are only of attendant importance. This statement is supported by our photos of the remaining material No. 3 in the container subjected mainly to compression under deformation. In this case, the texture anisotropy does not occur.

To make sense of the possible ways of how the dark and light regions are formed, their microstructure must be examined in more detail. First, it should be noted that the relative content of the boride grains in the light region is considerably higher, i.e., the dark regions are enriched with the metal binder. Second, the grain size in these regions is substantially different; in the dark region the grains are, on the average, more coarse and more elongated (Table 3). In addition, in the dark regions the grains are mainly oriented in the material flow direction. The relative number of the grains oriented at an angle of $\leq 45°$ to the extruded rod axis has been estimated. The content of the thus oriented grains is $\approx 60\%$ for material No. 1 and $\approx 80\%$ for material No. 2 of the total number of the elongated grains. Based on this, we may assume that increasing the binder content in the material facilitates the grain orientation in the material flow direction. In the light regions no grain orientation effect has been revealed.

From the analysis of all experimental data the following mechanism of forming the light and dark regions may be assumed. In extruding the porous material, the pore systems are oriented in the flow direction at the deformation place. Moreover, cracks can be formed between the layers under shear. The nickel binder rushes into these systems of pores and cracks if it is in a liquid state. Thus, shear deformation of the material may be considered to be the reason why the dark and light regions are formed. Supposedly, the binder-enriched regions are the places where shear deformation is concentrated. It facilitates the growth of the grains and their orientation.

Thus, the microstructure of materials having different binder content has been studied for the Hf–Ti–B–Ni system used as an example; the texture anisotropy of the materials having a binder content (30 and 40%) in the form of the light and dark regions elongated in the flow direction has been revealed; the microstructure of these regions with different content of the binder and different grain size has been described; a possible mechanism of their formation has been proposed; grain orientation in the material extrusion direction has been revealed in the dark binder-enriched regions.

The specific features mentioned of the microstructure of the system under study point to the possibilities of extrusion for forming the texture of refractory materials under deformation.

III. Grain Deformation and Anisotropic Effects (W–Ni–Fe System Used as an Example). In studying heavy alloy tungsten-base samples for SHS materials we have succeeded, for the first time, in revealing not only the orientation of grains in the material extrusion direction but also the deformation of these grains possessing sufficient plasticity.

The alloys of the W–Ni–Fe system are composed of tungsten crystallites surrounded by the binder–hard Ni–Fe–W solution [14].

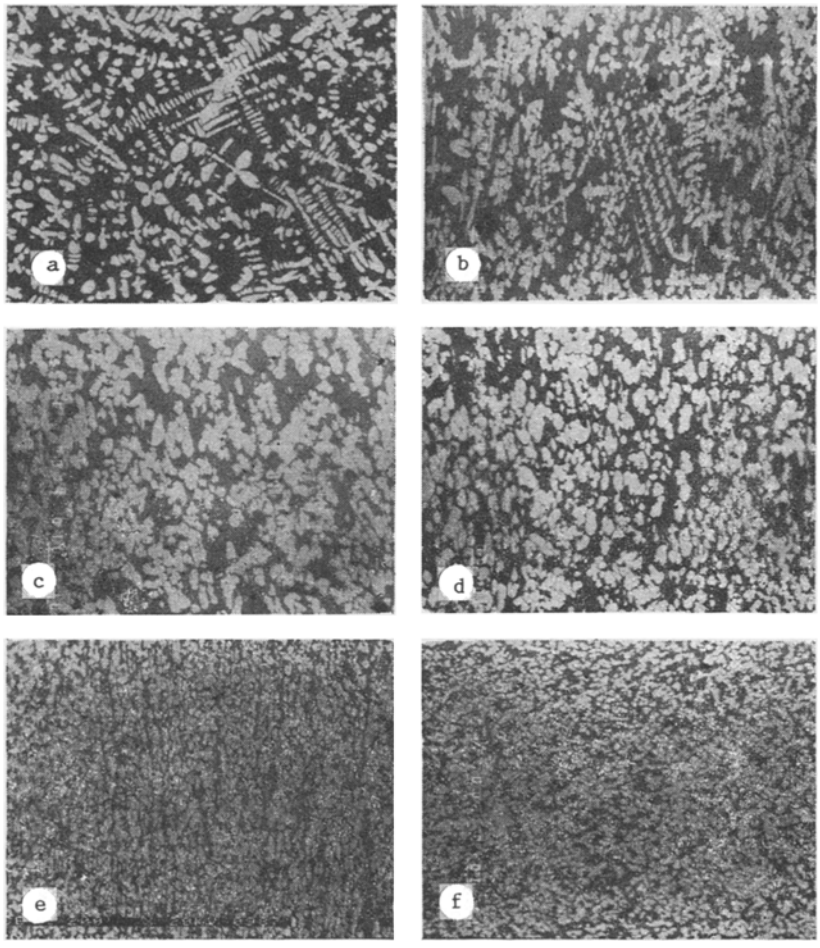

Fig. 11. Microstructure of the central part of the W–Ni–Fe alloy-containing samples extruded at different strain values: a) ψ = 0 (billet); b) 60%; c) 75%; d) 85%; e) 90%; f) ψ = 85% (across the grain). ×200.

The test samples have been fabricated by using one of the flow sheets adopted in SHS metallurgy [15], i.e., by smelting with tapping of a metal phase, at which the alloy overflows into another container. Upon crystallization the alloy has undergone extrusion and the strain value has varied from 60 to 90%. As the strain value increases, separate macropores disappear on the inlet part of the sample. The microstructure of the central part of the samples extruded with different strain values is shown in Fig. 11. The billet (Fig. 11a) has a structure composed of coarse dendrite grains having the developed axes without any orientation. At a strain value ψ = 60% (Fig. 11b) the samples partially retain the initial structure of the alloy; at ψ = 75% (Fig. 11c) the tungsten grains are oriented in the material flow direction at the deformation place which is most pronounced for ψ = 85% and, especially, for ψ = 90% (Fig. 11d, e). Grinding of dendrites up to the oval-shaped grains which are most uniformly located in the container is characteristic for the last two samples. It is characteristic that for SHS materials we have succeeded, for the first time, in observing not only the clear orientation of grains in the extrusion direction but also their deformation in the test system used as an example, i.e., the grains take on an elongated shape and their mean size decreases. Thus, the mean size of the grains decreases from 20 μm for the billet to 13 μm for the sample with ψ = 90% and for the thickness, from 10 to 65 μm, respectively. A difference in the microstructure of the length and cross cuts (Fig. 11d, e) is clearly seen for one and the same sample with ψ = 85%. The mean size of the grains is length 10 μm and thickness 7 μm. The microhardness of the hard solution-binder and tungsten grain amounts, on the average, to 3.51 and 5.70 GPa, respectively.

Thus, the present work has described some specific features of the structure formation of extruded refractory compound-base materials. Of these specific features we have distinguished:

– orientation of the pore systems in the material flow direction;

– grain orientation in the extrusion direction and texture formation under deformation;

– deformation and failure of grains possessing sufficient plasticity.

All these effects are caused by the shear deformation contribution. These have been found on different objects: composite refractory titanium carbide-, titanium boride-, hafnium boride-, and tungsten-base materials, which are not universal in nature. Evidently, the experimentally marked specific features of the material structure formation do not exhaust all the possibilities of the shear deformation contribution under SHS extrusion conditions. It may be expected that integrated studies in this direction will enable one to improve the service properties of the metal–ceramic article.

NOTATION

ψ, strain value; d_0, initial workpiece diameter; d_1, extruded article diameter; d_{av}, mean size of the TiC grains; R, sample radius, Θ, microporosity of the sample; l, length of the extruded part; η_{eff}, effective viscosity of the extrusion moment; Δt, material deformation time under pressure; sec; L, distance from the top of the remaining part of the material to the outlet eye of the container, mm; V, volume of the material extruded through the outlet eye of the container for time Δt, mm^3; σ, bending strength.

LITERATURE CITED

1. A. G. Merzhanov, Self-Propagating High-Temperature Synthesis: Twenty Years of Searches and Findings [in Russian], Preprint of ISMAN Chernogolovka (1989).
2. V. P. Severdenko, M. I. Kalachev, and P. P. Ankut, Plasticity and Plastic Metal Working [in Russian], Minsk (1968), pp. 13-17.
3. H. L. Piu (ed.), Mechanical Properties of Materials under High Pressure [Russian translation], Vol. 1, Moscow (1973).
4. D. K. Bulychev, B. I. Beresnev, M. G. Gaidukov, et al., Fiz. Met. Metalloved. **18**, No. 3, 433-438 (1964).
5. B. I. Beresnev, K. I. Ezerskii, and E. V. Trushin, Physical Fundamentals and Practical Use of Hydroextrusion [in Russian], Moscow (1981).
6. V. P. Severdenko, V. S. Muras, and A. P. Chelyshev, Plasticity and Plastic Metal Working [in Russian], Minsk (1968), pp. 143-147.
7. B. M. Khusid, Rheophysics and Thermophysics of Nonequilibrium Systems [in Russian], Pt. II, Minsk (1991), pp. 3-10.
8. A. G. Merzhanov, I. P. Borovinskaya, M. D. Nersesyan, S. O. Mkrtchyan, and T. B. Avakyan, Dokl. Akad. Nauk SSSR, **305**, No. 3, 1375-1378 (1988).
9. A. S. Rogachev, V. M. Shkiro, I. D. Chausskaya, and M. V. Shvetsov, Fiz. Goreniya Vzryva, No. 6, 86-93 (1988).
10. K. S. Chernyavskii, Stereology in Metal Science [in Russian], Moscow (1977).
11. L. S. Stelmakh, Heat and Mass Transfer in Chemically Reactive Systems, Proc. Intern. School Seminar [in Russian], Pt. 2, Minsk (1989), pp. 21-30.
12. A. G. Merzhanov, A. M. Stolin, et al., A Method of Making Articles from Powder Materials and a Device for Making Them. International Application PST/SU 88/00274 as of 20.12.88.
13. A. G. Merzhanov, G. Yu. Shekk, et al., Dokl. Akad. Nauk SSSR, **310**, No. 6, 1366-1370 (1990).
14. C. G. Li and R. M. German, Int. J. Power Metall. Power Technol., **20**, No. 1, 149-162 (1984).
15. V. I. Yukhvid and V. I. Ratnikov, Process Designs and Equipment in SHS Metallurgy [in Russian], Preprint of ISMAN, Chernogolovka (1989).